Proceedings of the 28th IEEE
EMBS Annual International Conference
New York City, USA, Aug 30-Sept 3, 2006

An Artificial Nano-Drainage Implant (ANDI) for Glaucoma Treatment

Tingrui Pan, *Student Member, IEEE*, J. David Brown, and Babak Ziaie, *Member, IEEE*

Abstract—**Glaucoma is the leading cause of irreversible blindness. The loss of sight in glaucoma is due to the permanent optic nerve damage which is the result of a chronic elevated intraocular pressure. In this paper, we report a completely new concept to treat glaucoma using a nano-drainage device fabricated through MEMS and nanofabrication technologies. This involves replacing the functionality of diseased drainage pathway for aqueous humor outflow (*i.e.*, trabecular meshwork). By enhancing aqueous humor outflow, the artificial drainage implant will lead to a decrease in the intraocular pressure and a halt in the progression of glaucoma.**

Index Terms—**Aqueous humor, artificial drainage, biofluidics, glaucoma, MEMS, nanofabrication.**

I. Introduction

Glaucoma is the leading cause of irreversible blindness worldwide. The number of people with glaucoma is nearly 70 million, and more than 10% of them are bilaterally blind. In the United States alone, 2.2 million people have glaucoma. This number is expected to increase by 50% by 2020 due to the aging population (glaucoma prevalence increases markedly with age) [1]. Glaucoma-induced blindness is the result of permanent damage to the optic nerve due to an increased intraocular pressure (IOP). According to a Mayo Clinic study, there is a 54% risk of blindness with glaucoma after 20 years, even with treatment [2], which implies that current glaucoma treatment methods are not fully effective. Improving the aqueous humor outflow can lead to a decrease in the IOP. In this paper, we report an entirely new concept to treat glaucoma using the emerging MEMS and nanofabrication technologies, which involves replacing the diseased drainage pathway (*i.e.*, the trabecular meshwork) [3]. A schematic of the artificial nano-drainage implant (ANDI) is shown in Figure 1. It consists of a nanoporous membrane (mimicking the drainage function of the trabecular meshwork) connected to an integrated polymeric shaft inserted through the sclera into the anterior chamber, thereby, allowing a bypass route for the aqueous humor outflow. We will describe the design, fabrication, and initial test results on the above nano-drainage device in the following sections.

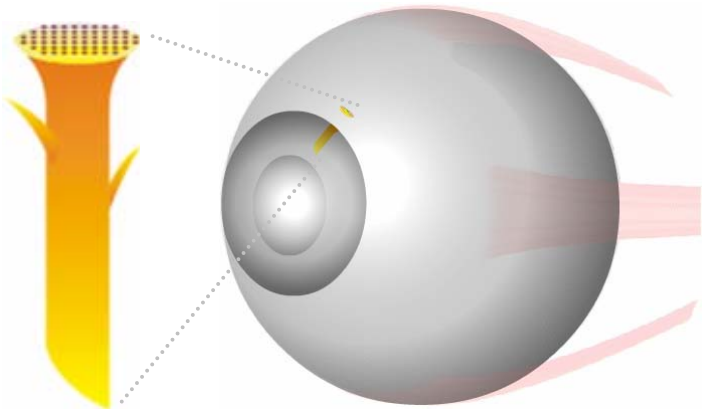

Fig 1. Schematic of an artificial nano-drainage implant for glaucoma treatment.

II. Design and Fabrication

All current glaucoma drainage devices consist of a polymeric tube inserted into anterior chamber and terminated in a back-plate implanted under conjunctiva. These devices, although clinically useful to some extent, have several severe drawbacks such as inadequate long-term pressure management and post-operative hypotony. The idea of bypassing the clogged trabecular meshwork by a nanoporous membrane was initially suggested in the 1980s. However, initial studies of aqueous humor perfusion through such membranes showed protein plugging as a result of hydrophobic interactions [4]. Myocilin, a strongly hydrophobic protein, was identified as being the likely cause of that obstruction [5]. An artificial trabecular meshwork without protein obstruction has been a fanciful goal of ophthalmologists since these initial pioneering experiments. Nowadays, emerging MEMS and nanofabrication technologies make this idea promising and practical.

Manuscript received April 3, 2006. This work was supported in part by the National Science Foundation under CAREER award BES-0093604 to Dr. B. Ziaie and by the University of Minnesota Doctoral Dissertation Fellow to Dr. T. Pan.

Tingrui Pan is with the Department of Ophthalmology, University of Minnesota, Minneapolis, MN 55455, USA (phone: 612-625-7353; fax: 612-626-3119; e-mail: tingrui@umn.edu).

J. David Brown is with the Department of Ophthalmology, University of Minnesota, Minneapolis, MN 55455, USA (e-mail: brown008@umn.edu).

Babak Ziaie is with the School of Electrical and Computer Engineering, Purdue University, West Lafayette, IN 47907, USA (e-mail: bziaie@purdue.edu).

As shown in Figure 1, the current nano-filtration implant design could easily and safely be inserted into a glaucomatous eye and could immediately and predictably lower the IOP. However, since the implant is exposed to the external environment, it has to prevent bacterial ingression. Water purification studies have shown that a nanopore of 200nm or less in diameter can effectively prevent bacterial penetration. The tiny porous size will contribute to protein adsorption and clogging unless a non-fouling biocompatible material is coated on the surfaces [6]. Moreover, an integrated packaging technique has to be utilized to connect the filtration membrane to a polymeric shaft for an easy implantation procedure.

Table 1. Membrane design parameters.

Membrane Design Parameters	
Membrane Thickness (***L***)	600nm
Nanopore Radius (***r***)	100nm
Flow Resistance (***R***)	1.711×10^{19}Pa·sec/m^3
Physiological Flow Rate (***Q***)	4.5×10^{-11}m^3/sec (2.7μL/min)
Target Pressure (***ΔP***)	1600Pa (12mmHg)
Number of Pores (***N***)	~500,000

Fluidic resistance of a single nano channel, at the laminar flow regime can be estimated through the *Poiseuille's* equation [7],

$$R=\Delta P/Q=8\mu L/(\pi r^4)$$

where μ is the viscosity of the fluid, and L and r are the length and radius of the cylindrical pore. As shown in Table 1, the current design has a membrane thickness of 600nm and pore radius of 100nm. Therefore, roughly half a million nanopores are needed to set the IOP at 12mmHg assuming a physiological aqueous humor flow rate of 2.7μl/min. The dimensionless *Reynolds* number (*Re*), correlating the viscous behavior of all Newtonian fluids, is described as

$$Re=\rho VL/\mu$$

where V and L are characteristic velocity and length scales of the flow, and ρ and μ are the density and viscosity of the fluid. According to the current design parameters, $Re = 1.4\times10^{-9} << 1$, which indicates that flow in the nanopores is highly viscous and therefore the *Poiseuille's* equation can be a good estimation in this case. In order to increase the mechanical strength of the nanoporous membrane, the total area is divided into smaller ones separated and reinforced by rigid full-wafer anchors.

Figure 2 shows the fabrication process for the ANDI along with its integrated packaging outlet. The process starts with a 6000Å low-stress silicon nitride deposited on a silicon wafer using low-pressure chemical vapor deposition (LPCVD). It continues with a backside patterning of the nitride layer followed by the deep reactive ion etching (DRIE) of a group of microscale fluidic accesses ($40\times40\mu m^2$) to the filtration membranes. Meanwhile, multi narrow concentric rings around the fluidic access are also machined at the same step. Due to the DRIE lag effect, these smaller rings do not penetrate all the way throughout the silicon thickness [8] (Figure 2-a). A subsequent isotropic reactive ion etching (RIE) step removes the thin sidewalls between these multi concentric rings and creates a flange-shaped packaging socket for the tube connection (Figure 2-b). A photodefinable polymethyl methacrylate (PMMA) is then used as the imaging layer to pattern a large array of the nanopores using electron-beam lithography (Raith GmbH, Germany). Here, the wafers are cleaned in isopropyl alcohol prior to application of the PMMA layer. 950 PMMA C4 (MicroChem Corp., MA) is spun on top of the substrate for a 50sec of spinning at 1200rpm. Subsequently, a prebake step is performed for 75sec at 180°C on top of a hot plate. Although the theoretic curve predicts a thickness of 7000Å can be obtained at this condition, we reproducibly achieved a film thickness of 6000Å. The patterns are then exposed to the electron beam at a dose level of 0.10fC (the bias voltage of 20kV and aperture size of 30μm). PMMA is then developed using methyl isobutyl ketone (MIBK) for 45sec followed by a 60sec rinse in isopropyl alcohol (IPA). In order to obtain different tapered angles in the pore cross section profile, concentration of a compound developer composed of MIBK and IPA was adjusted accordingly. A final hard bake step at 120°C for 2min is required prior to the nitride RIE step (SF_6:O_2 is 20:20sccm, chamber pressure is 25mtorr, DC plasma voltage is 125V, and the temperature is maintained at 5°C), Figure 2-c, d. At the end of the process, a frontal etching is finally used to release the nanoporous filtration device with the fluidic connector. For packaging, a medical-grade heat-shrink tube is used to seal the fluidic connection at 143° without using any adhesive [9]. Figure 3 shows scanning electron microscopic (SEM) photographs of (a) a backside cross-sectional view of the nanoporous drainage implant and (b) a frontal close-up view of a silicon nitride nanoporous membrane suspended over the fluidic access.

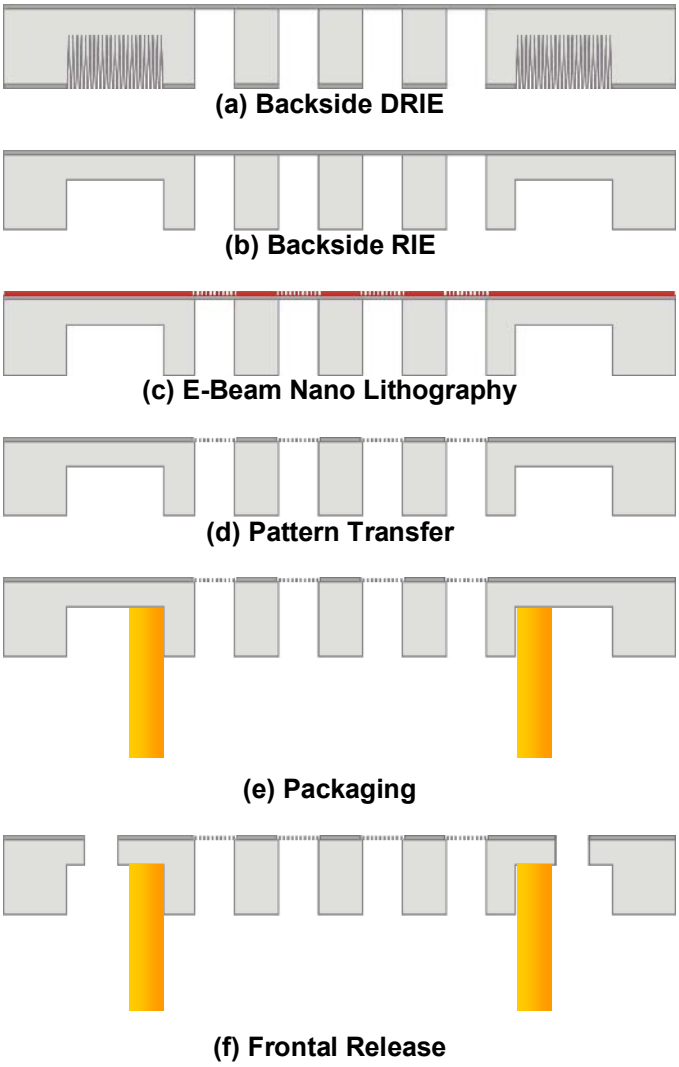

Fig 2. Fabrication process for the ANDI. (a) backside DRIE, (b) backside RIE, (c) electron-beam nano lithography, (d) pattern transfer, (e) packaging, and (e) frontal release.

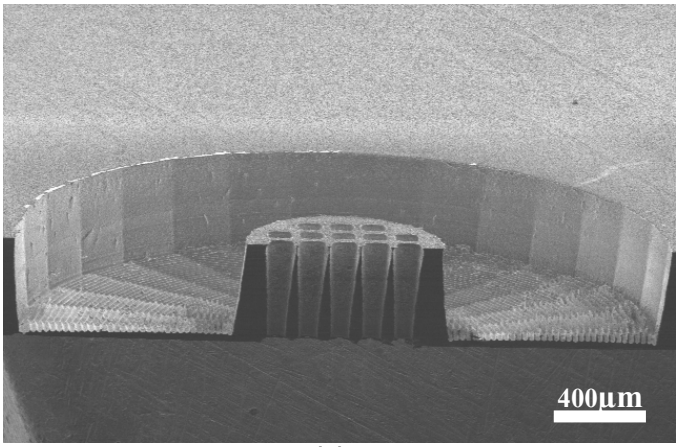

(a)

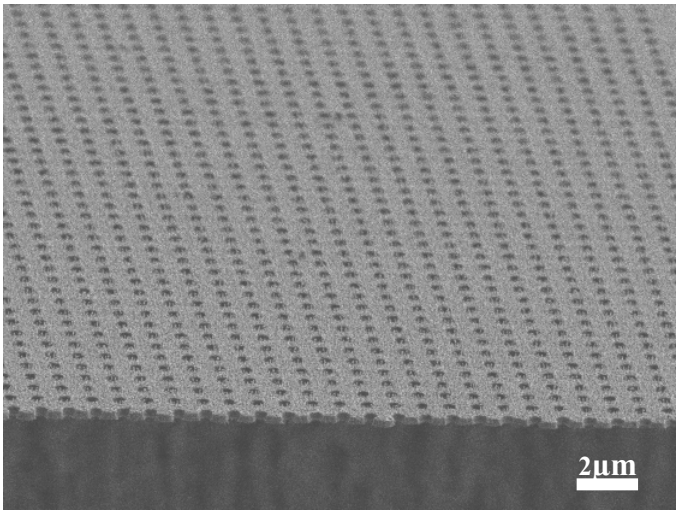

(b)

Fig 3. Scanning electron microscopic (SEM) photographs of (a) the backside cross-sectional view of the implant and (b) the frontal close-up view of a silicon nitride nanoporous membrane suspended over the fluidic access.

As can be seen, the pores are tapered to minimize the flow resistance with a top opening of 400nm and a bottom opening of 200nm in diameter. The tapered design achieved by adjusting the RIE condition can significantly bring down the fluidic resistance by a factor of 2-4. Figure 4 shows the finite element simulation results of the fluidic resistance in nanopores with different tapering angles. The tapered profile allows for a design with fewer number of pores and smaller membrane area, *i.e.*, miniaturizing the device dimensions further.

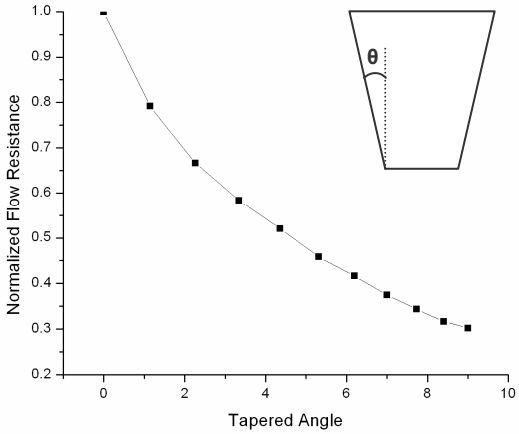

Fig 4. Flow resistances in nanopores with different tapering angles

III. Results and Future Work

Figure 5 shows a prototype of our nanoporous glaucoma implant packaged by a medical heat shrink tubing (1.5mm in diameter and 4mm in length). This could potentially provide a safer, more effective, and less expensive treatment for glaucoma, and would also certainly have broader applications in other medical fields.

Fig 5. A prototype of our nanoporous glaucoma implant packaged by a medical heat shrink tubing.

An *in vitro* microfluidic setup is used to characterize the nanoporous implants [10]. These tests are performed at room temperature using saline and saline diluted plasma solutions (plasma/saline ratio of 1:300 having the same protein level as the aqueous humor, *i.e.*, 0.024g/100ml [11]) at the physiological aqueous humor flow rate of 2.5µl/min. Figure 6 shows the constant-flow test results using a syringe pump. As expected, the nano filtration membrane provides the designed flow resistance to the saline flow, while cross-linking and clogging of proteins inside the nanopores from plasma perfusion significantly increases the flow resistance.

Our future efforts will focus on applying surface chemistry modification to the nanoporous membrane, both on the surface and along the pore sidewalls. Water plasma treatment could be used to create silanol (SiOH) groups on the silicon nitride surface with a uniform coverage. Then, a low molecular weight (M_w) PEG coating could be applied to the nanoporous surface through chemical vapor deposition. PEG is then grafted onto the silanol groups through the formation of an ester bond. Such surface modifications will be tested and will indicate whether or how fast proteins from aqueous humor might clog the nanopores.

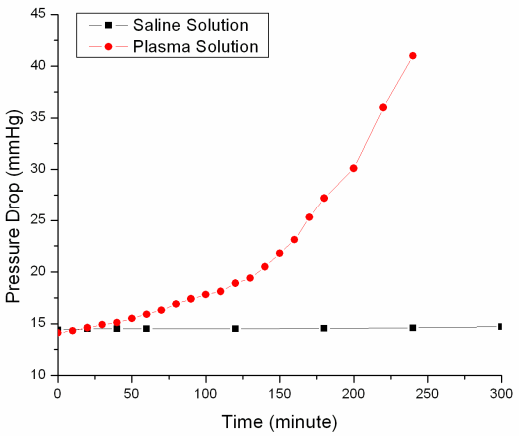

Fig 6. Constant flow test results

Acknowledgment

The authors would like to thank Dr. E. Aydil in the Department of Chemical Engineering and Materials Science at the University of Minnesota for valuable discussions and suggestions in surface chemistry modification.

Reference

[1] National Eye Institute, http://www.nei.nih.gov.
[2] M. G. Hattenhauer, *et al.*, "The Probability of Blindness from Open Angle Glaucoma," *Ophthalmology*, vol. 105, pp. 2099-2104, 1998.
[3] M. B. Shields, *Textbook of Glaucoma*, 1998.
[4] M. Johnson, *et al.*, "The Flow of Aqueous Humor through Micro-Porous Filters," *IOVS*, vol. 27, pp. 92-97, 1996.
[5] P. Russell, *et al.*, "The Presence and Properties of Myocilin in the Aqueous Humor," *IOVS*, vol. 42, pp. 983-986, 2001.
[6] C. R. Ethier, *et al.*, "Calculations of Flow Resistance in the Juxtacanalicular Meshwork," *IOVS*, vol. 27, pp. 1741-1750, 1986.
[7] W. K. McEwen, "Application of Poiseuille's Law to Aqueous Outflow," *Archives of Ophthalmology*, vol. 60, pp. 290-294, 1958.
[8] B. A. Parviz and K. Najafi, "A Geometric Etch-Stop Technology for Bulk Micromachining," *Journal of Micromech. Microeng.*, vol. 11, pp. 277-282, 2001.
[9] T. Pan, A. Baldi, B. Ziaie, "A Reworkable Adhesive-Free Interconnection Technology for Microfluidic Systems," *JMEMS*, vol. 15, pp. 267-272, 2006.
[10] T. Pan, *et al.*, "Modeling and Characterization of a Valved Glaucoma Drainage Device with Implications for Enhanced Therapeutic Efficacy," *IEEE Trans. on Biomedical Engineering*, vol. 52, pp. 948-951, 2005.
[11] R. Ritch, M. B. Shields, and T. Krupin, *The Glaucomas: Basic Sciences*: Mosby, 1996.